Silicon (2022) 14:8205–8222
https://doi.org/10.1007/s12633-021-01584-5

ORIGINAL PAPER

A Low Thermal Conductivity of Lightweight Laterite-cement Composites with Cotton Wastes Fibres

Van Essa L. Kamga. Samen[1,2] · Juvenal Giogetti Deutou Nemaleu[1] · Rodrigue Cyriaque Kaze[1,3] · Franck Docgne Kammogne[2] · Pierre Meukam[2] · Elie Kamseu[1,4] · Cristina. Leonelli[4]

Received: 31 August 2021 / Accepted: 29 November 2021 / Published online: 9 January 2022

Abstract

The development of eco- friendly environmental and sustainable building materials having low thermal conductivity and optimal physic-chemical abilities ensuring passive thermal comfort is imperative in the global quest for the minimization of greenhouse-gases (GHG) emission and energy needs in homes. To attend this objective, the present work underlines the feasibility of using waste cotton fibres for the design of the lightweight laterite-cement composites with low thermal conductivity for structural applications. The final products were obtained by replacing laterite cement composite with cotton wastes fibres (0.3-0.6 wt%) and then uniaxial pressing around 14 MPa. The thermo-engineering and structural properties were performed using several techniques: X-Ray Diffraction (XRD), Environmental Scanning Electron Microscope (ESEM), Fourier Transform Infrared Spectroscopy (FTIR), mechanical properties as well as thermal conductivity. This process accounts for the optimum (0.78 $W.m^{-1}. K^{-1}$) structural material made with 6 wt% cement, 0.6 wt% cotton fibres and better packing density of laterites particles (50/50). Regardless of the particle size distribution of aggregates (laterite), the increase of cotton fibres content resulted in lowering mechanical performances. This is due to the creation of pores and the weakness adhesion between the cellulosic fibres and laterites particles within the matrix. In addition, the presence of cellulose within a matrix enhanced the crystallinity of cementitious phases (CASFH and CASH) of the end-products. The formulated samples with the reduction around 29% of embodied energy compared to the conventional materials, appears as a promising eco-friendly composite with good thermal comfort, small-embodied energy and low environmental impact through sustainable process.

Keywords Laterites · Cotton fibres · Thermal performances · Embodied energy · Microstructure

1 Introduction

Thermal comfort is one of the major concerns in building construction. The most common methods of dealing with are generally electrical air regulating methods such as air conditioners, heaters and ventilators [1, 2]. However, the implementation of these artificial methods of regulation has a direct consequence on energy consumption and the production of greenhouse gases, the main responsible of global warming. Building sector consumes 32% of primary energy, about 40% of the world's energy and is responsible for almost 33 – 40% of greenhouse gas emissions [3, 4]. Then, building sector becomes the main target for reducing energy consumption [5]. For example, air conditioners and ventilators are responsible of about 10% of the world electricity and the number of air conditioners all over the world could increase from 1.6 billion today to 5.6 billion at 2050 [6]. These statements drawback the Paris Agreement

✉ Van Essa L. Kamga. Samen
liliane.sk16@gmail.com

✉ Juvenal Giogetti Deutou Nemaleu
giogetti@live.fr

✉ Elie Kamseu
kamseuelie2001@yahoo.fr

1 Local Materials Promotion Authority (MIPROMALO), P.O. Box 2396, Yaoundé, Cameroon

2 Laboratoire Eau, Energie, Environnement, Ecole Nationale Polytechnique de Yaoundé, P.O. Box 8390, Yaoundé, Cameroon

3 Laboratory of Applied Inorganic Chemistry, Faculty of Science, University of Yaoundé I, P.O. Box 812, Yaoundé, Cameroon

4 Department of Engineering Enzo Ferrari, University of Modena and Reggio Emilia, Via Vignolese 905/A, 41 125 Modena, Italy

limiting global warming to +1.5 °C at 2050 [7–9]. It becomes urgent to develop eco-friendly and sustainable building materials having with low thermal conductivity and optimum physico-chemical abilities to ensure passive thermal comfort without electric conditioner. Several materials capable to ensure thermal insulation already exist. The most used until now are ice fibres, mineral wool and foam insulation materials based on polymers compounds [10–12]. However, their manufacture still requires a lot of energy and even have environmental limits [13]. Recently, a new technique of insulation has been introduced by researchers such as vacuum insulating materials [14, 15], aerogels [16] and composites that are characterized by their heat reflection and storage [12, 17]. These techniques also present some limits because the manufacture of the final insulating materials is linked to the transformation of fossil resource such as oil and bauxite, which not only generate greenhouse gases but also have an important energy demand [18, 19]. The improvement of the energy efficiency of building must not only involve the thermal insulation of the building envelope, but also the reduction of grey energy for the building material. For all the above reasons, the traditional thermal insulation is coming back in order to develop material from renewable resources [20–23].

Composites derived from natural resources still remains the best approach because of their low cost, availability and good thermal properties [24]. These included the use of rice and wheat husk [21, 25], rice straw [26], sawdust [27], waste paper [28], as well as cotton waste [29]. Several studies were conducted taking into account the aforementioned characteristics. For example, Saghrouni et al. [30] studied the incorporation of Juncus maritimus fibres in mortar composites at different dosages. He succeed to reduce of about 65% the thermal conductivity at 10% fibre addition in the composite which reaches 0.182 $W.m^{-1}.K^{-1}$ while it equivalent is about 2.8 $W.m^{-1}.K^{-1}$ without any addition. Previously, Belhadj et al. [31] made concrete lightened by the addition of barley straws. These authors claimed that the manufactured concrete showed a reduction in compressive strength with the fibres added and an improvement of flexural strength and other properties such as lightness, deformability, ductility, toughness and thermal characteristics (1.32 $W.m^{-1}.K^{-1}$).

Cotton fibres has equally proved their efficiency in the production of thermal insulation materials. Halil et al. combined cotton, limestone wastes and Portland cement with calcite to produce new low cost and lightweight composite as a building material. The process of curing was into a tank filled with lime-saturated water at 22 °C during 28 days before drying with a ventilated oven at 105 °C. The results showed that this new composite is about 60% lighter than the conventional concrete brick (cement-sand concrete) with mechanical properties that satisfy the requirements for building materials.

On the other hand, Alomayri et al. [32] have rather studied the effect of cotton addition in a geopolymer matrix-based fly ash on the physical, mechanical and fracture behaviours. They found that the mechanicals properties of geopolymers composites increase up to 0.5 wt% of cotton fibres content. Beyond that percentage, these properties drop while the density decrease regardless the fibres content. The lowest density is observed with an addition of 1 wt% of cotton fibres (1.8 g. cm^{-3}).

Although these different developed materials are capable to achieve a good thermal comfort, there are not always environmentally friendly [13]. In addition, there is a lack of data concerning cotton waste within laterite-cement composites. In general, cotton fibre waste is recovered for the production of lightweight materials used as building panel [33, 34]. However, structural materials with low thermal conductivities can be develop in order to implement a building material without having to develop a multi-layer construction. In the case of fired bricks, the process used is the development of cells inside the brick [35] while the stabilization with fibres is indicated in the case of laterite-cement composites. The reflection on the composite laterite cotton fibre is based on the principle that cotton fibres will break the chain of thermal conductivity that is potentially important in laterite with the presence of iron minerals. However, laterite is a raw material abundant in tropical area [36, 37] and has the particularity that many other raw materials do not have. The ability to react directly with the cement or to be activated without treatment with acid or alkaline solutions [38, 39]. Thus, the objective of this project can be perceived on three levels: on the environmental level with the reduction of greenhouse gas emissions due to the green process used for the establishment of the new eco-composite, on the energy level with the reduction of energy demand not only during the development of the material but also during its use. Finally, the motivation of this work is to develop a rather original and ecological solution to meet the requirements of the standards while maintaining a low thermal conductivity.

Density, porosity and water absorption are uses together with the mechanical properties (flexural and compressive strength) to assess the efficiently of laterite-cement composite achieved to act as structural building material. Fourier Transform Infrared Spectroscopy (FT-IR), Environmental Scanning Electron Microscope (ESEM) as well as X-Ray Diffraction (XRD) are used to investigate on the phase's evolution and microstructure.

2 Materials and Experimental Methods

2.1 Materials and Samples Preparations

The mainly precursors used is the iron-rich aluminosilicates (laterite) having 37.5 wt % of Fe_2O_3, 25.1 wt% SiO_2 and 23

wt% of Al_2O. This percentage of iron shows that this laterite is a corroded kaolinite and belongs to the class of Silicate laterites according to Tuncer [40] or could be classified as true lateritie ($R < 1.33$) according to some researchers [41] which classified iron rich alluminosilicates based on the ratio of silica/sesquioxides $R = SiO_2/(Al_2O_3 + Fe_2O_3)$. After grinding, the laterite was dried, crushed and then sieve in two fractions: the fine particles series which are considered as binding phases ($\varphi \leq 1$mm) and coarse particles size ($1\text{mm} \leq \varphi \leq 4\text{mm}$), which are inert and do not really participate in the development of pozzolanic reactions. The cement used was a Ordinary Portland Cement (CEM II 42.5) from Dangote cement factory, Douala Cameroon. This cement contains clinker, gypsum and pozzolan. The minerals phases of laterites are quartz, kaolinite, hematite, goethite, anatase, and lepidocrocite [42] while CEM II 42.5 presented : Alite, Belite, quartz, calcite, pyroxene and plagioclase [43, 44]

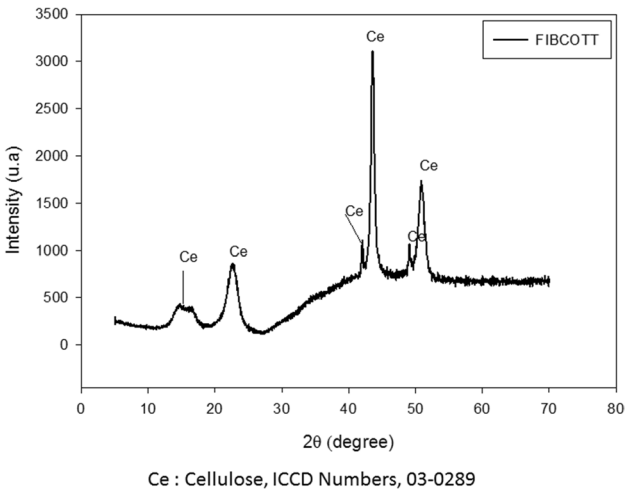

Fig. 1 XRD patterns of waste cotton fibres

(Table 1). The cotton waste used come from the Sodecoton factory. The diffraction pattern of waste cotton fibres shows typical characteristic peaks, indicating the presence of cellulose (Fig. 1) as some researchers found [45]. The bulk chemical composition of the cotton waste is recorded in Table 2. Two powders of different fines/coarse ratio (75/25, 50/50) were prepared. The fine particle series corresponds to laterite seeds with a diameter smaller than 1mm ($\varphi \leq 1$mm; including nano and micro particles) (Fig. 2a) whereas that of the coarse particles comprises seeds of laterites whose diameter varies from 1 mm to 4 mm ($1\text{mm} \leq \varphi \leq 4\text{mm}$) (Fig. 2b). To each powder 6 and 8 wt% of cement were added. The amount of water added to each formulation before pressing varied from 12.5 to 15 vol% according to the fines content. The more material contains fine particles, the more water is absorbed. The powder 75/ 25 received 15 vol% of water while 50/50 received 12.5 vol%. In order to have homogenous dispersion of the fibre, the cotton fibres are added under stirring using the Hobart mixer (model N50_G) which ensured gradually mixed during 15 min. The mixture was then transferred into the mold (205mm x 95mm x 35mm), Nannetti Brand press machine, and pressed up to 140 bars. The total mass of the mix of one specimen was 1400 g for each formulation. LYZ is the general designation of the formulations achieved. L_{75} and L_{50} refer to the two granulometries identified; Y_6 and Y_8 give the percentage of cement while Z_0 to $Z_{0.6}$ refer to the cotton waste content (Table 3).

The curing process was carried out in two stages. The samples were first wrapped into plastic for the first 28 days in order to avoid water evaporation and then, the curing continued under normal laboratory conditions to promote contact with the air in order to ensure better pozzolanic reactions. The Fig. 3 shows a sample set after casting.

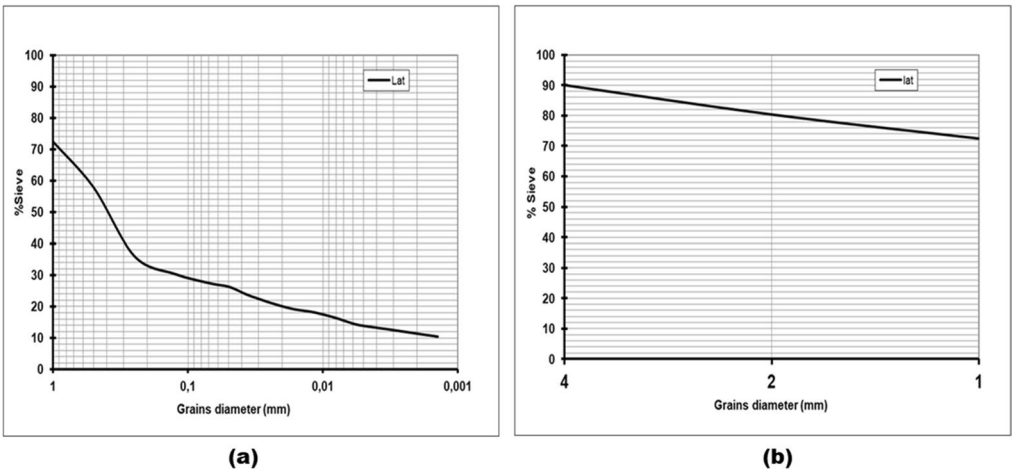

Fig. 2 Gradation curves of the laterite used: (**a**) fine aggregate and (**b**) coarse aggregate

Table 1 Chemical compositions of raw materials

Oxides (wt%)	Laterite	Ordinary Portland Cement (CEM II 42.5)
Fe_2O_3	37,5	4,65
SiO_2	25,1	19.3
Al_2O_3	23	5,5
TiO_2	0,9	/
V_2O_5	0,15	/
P_2O_5	0,14	/
Cr_2O_3	0,23	/
CaO	0.29	65
MgO	0.07	0,98
CaO free	/	1,8
K_2O	1.8	0.9
SO_3	Not detectable	2.01
Na_2O	0.2	0.2
LOI	10,6	0.45

Table 2 Bulk chemical analysis of cotton fibers [29]

Compositions	%
Cellulose	80 - 90
Hemicelluloses	4 - 6
Proteins	0 – 1.5
Waxes and Fats	0.5 - 1
Water	6 - 8

Table 3 Different mixtures of laterite-cement composite with addition of waste cotton fibers

	6 wt% of cement	8 wt% of cement		
75/25	$L_{75}Y_6Z_0$	$L_{75}Y_8Z_0$	0.0	Wt.% fibers
	$L_{75}Y_6Z_{0.3}$	$L_{75}Y_8Z_{0.3}$	0.3	
	$L_{75}Y_6Z_{0.4}$	$L_{75}Y_8Z_{0.4}$	0.4	
	$L_{75}Y_6Z_{0.5}$	$L_{75}Y_8Z_{0.5}$	0.5	
	$L_{75}Y_6Z_{0.6}$	$L_{75}Y_8Z_{0.6}$	0.6	
50/50	$L_{50}Y_6Z_0$	$L_{50}Y_8Z_0$	0.0	
	$L_{50}Y_6Z_{0.3}$	$L_{50}Y_8Z_{0.3}$	0.3	
	$L_{50}Y_6Z_{0.4}$	$L_{50}Y_8Z_{0.4}$	0.4	
	$L_{50}Y_6Z_{0.5}$	$L_{50}Y_8Z_{0.5}$	0.5	
	$L_{50}Y_6Z_{0.6}$	$L_{50}Y_8Z_{0.6}$	0.6	

2.2 Characterization Methods

2.2.1 Physico Mechanicals Test and Thermal Conductivity

The physico-mechanical tests (water absorption, bulk density and apparent porosity) were determined by Archimed's method using an electronic balance with a sensitivity of 10^{-3}. Before carrying the test, the samples were oven dried at 105 °C for 24 h to ensure that they were completely dry. Once removed from the oven, the samples were weighed one by one to determine dry mass (W_a). Then, they were soaked in water for 24 h. After this immersion, two masses of each sample were taken in two different conditions. The one just after the samples were removed from the water and the time to wipe with filter paper to remove surface water (W_r) and another while the sample was in the water (W_w).

Fig. 3 Photograph of a sample set after casting

Then, the water absorption, bulk density and apparent porosity can be calculated by the following equations.

$$\text{Water absorption } (\%) = \frac{W_r - W_a}{W_a} \times 100 \quad (1)$$

$$\text{Apparent porosity } (\%) = \frac{W_r - W_a}{W_r - W_w} \times 100 \quad (2)$$

$$\text{Apparent density } (g.m^{-3}) \frac{W_a}{W_r\text{-}W_w} \times \rho(\text{water}) \quad (3)$$

The physico mechanical test were performed following as well as possible the American Standard regarding the Standard Test method regarding water absorption, bulk density and apparent porosity [46].

As for the thermal conductivity, its determination was made thanks to the Hot Disk Thermal Constants Analyser. It is an emerging technology that uses the transient plane source technique to measure the in-plane and through-plane thermal conductivity of an anisotropic material in the same test. The sensors used in this test method consisted of a 10 µm thick nickel foil embedded between two 25.4 µm thick layers of Kapton polyimide film. The nickel foil was wound in a double spiral pattern and had a radius, R of either 3.189 mm or 6.403 mm. The thermal conductivities were measured at 23°C.

2.2.2 Phase's Analyses and Microstructure

FTIR analysis allows to identify bonds with the help of the corresponding wave number, to determine the characteristic groups and to highlight the hydrogen bonds. The spectrometer used for this analysis in the case of this work is the Nicolet 6700. It is equipped with a MCT (Mercury-Cadmium-Telluride or HgCdTe) detector and a potassium bromide (KBr) separator. The absorption spectra were obtained by adding 100 interferograms for each spectrum and were reproduced in the region from 4000 cm^{-1} to 400 cm^{-1}. They were recorded with a resolution of 2 cm^{-1}. The samples used for this test come from the breaks resulting from the determination of the mechanical properties and were ground finely under 80 µm before analysis. Each sample was placed over a reflective crystal medium where light passed through. A minimum of 32 scans were averaged for each spectrum at the intervals.

Laterite cement composites with the addition of waste cotton fibres aged of 90 days were crushed and sieved through a sieve of mesh 80 µm. These powders were then used in an X-ray powder diffractometer, XRD, (PW3710, Phillips) Cu Kα, Ni-filtered radiation (the wavelength was 1.54184 Å) in order to study the mineralogical phases. Each analysis was performed on ground samples and the radiation was generated at 40 mA and 40 kV. Random powder specimens were step-scanned from 5° to 70°, 2 Theta range, and integrated at the rate of 2 s per step. The crystalline phases were identified by comparison with tabulated data on the JCPDS files.

The morphology of the studied composites was examined by Environmental Scanning Electron Microscope (ESEM, Quanta200, FEI). These samples, resulting from the mechanical tests, were dried and cut parallel to fracture surface with the diamond saw to observe the fractures surfaces. In order to ensure a good analysis, these samples were covered with a thin layer of gold before be placed in a vacuum chamber on silver plates. Three ESEM micrographs were taken for each specimen in order to study the cellular structure.

2.2.3 Mechanical and Physic-chemical Properties

For the three-point flexural, the machine (ELE International machine) had the load rate fixed at 3 $mm.min^{-1}$. Three samples of dimensions 205 × 90 ×35 mm were placed between two supports at a distance of 150 mm according to the American Standard regarding the three-point flexural strength testing, ASTM C78/C78M − 18 5 [47].

The formula of mechanical flexural strength is given by the Eq. (4):

$$\sigma = \frac{3 \times 150F}{2 \times 90 \times 35^2} \tag{4}$$

Where σ is the maximum centre tensile stress (MPa), F maximum load at fracture (N), 150 mm is the distance between the supports, 90 mm is the width and 35 mm is the thickness of the specimen. The Fig. 4 shows respectively the photograph during the flexural test of the specimens (4a), the failure pattern observed (4b) and the interior of a moulded brick containing the fibres after flexural test (4c).

Concerning the compressive strength, the same machine was used and the dimensions of the six samples used for each specimen were 205 × 90 × 35 mm. These samples were compressed under a square surface of section 40 × 40 mm^2 according to the standard ASTM D695 ASTM C 39/C 39 M – 05 (2008) [48].

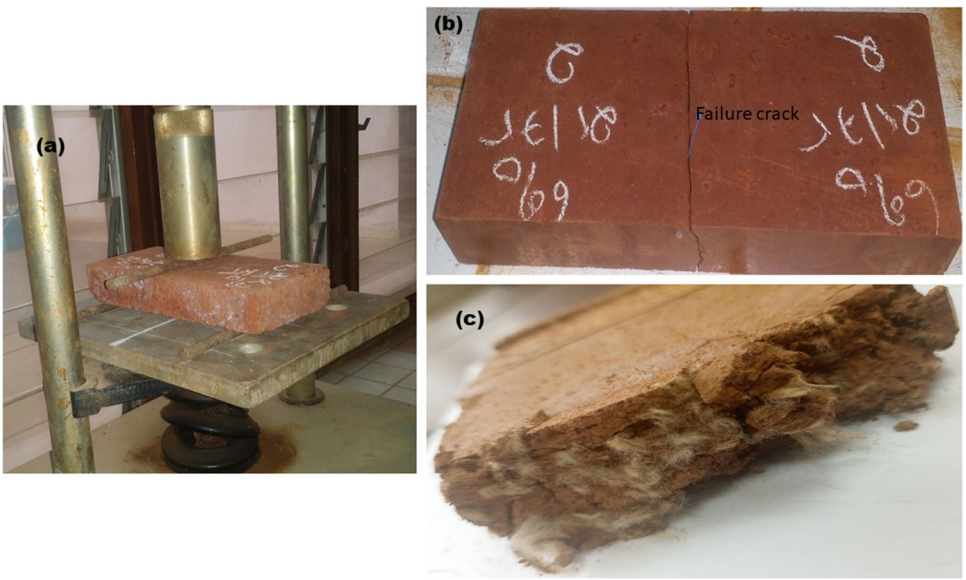

Fig. 4 Photograph of specimen during flexural test: (**a**) Setup, (**b**) Failure crack observed and (**c**) Overview of a broken brick

The formula of mechanical compressive strength is given by the Eq. (5):

$$R_c = \frac{F}{hxl} \quad (5)$$

Where Rc is the compressive stress (MPa), F the load of crushing (N), l the width and h the thickness of the specimen (mm).

3 Results

3.1 Physico Mechanical Properties

Table 4 summarized the density and porosity of the samples at 6 and 8 wt% of cement contents. $L_{50}Y_8Z_{0.3}$ has a porosity of 31.66% with a bulk density of 1.95 kg/m^3 while $L_{50}Y_8Z_{0.6}$ has a porosity of 32.07% with a bulk density of 1.82 kg/m^3. In addition, $L_{75}Y_8Z_{0.3}$ and $L_{75}Y_8Z_{0.6}$, have porosities equal to 32.43% and 33.12% respectively while their densities are1.67 kg/m^3 and 1.54 kg/m^3. As the bulk density decreases with the addition of the fibres, the porosity increases independently of the compositions. The same behaviour is observed with $L_{75}Y_6$ and $L_{50}Y_6$. Hence, incorporating the fibres in laterite-cement specimens made the materiel a bit light compared to the reference (laterite-cement without fibres) with a density equal to 2.13 kg/m^3 [4, 49]. These results are in agreement with those found by several other researchers who also found that the incorporation of fibres in composites decreases their density while increasing their apparent porosity [30, 31]. The main reason for the results found is that the cotton fibre waste has a much lower bulk density than laterite [4]. The substitution of any percentage of laterite by these fibres will make the matrix lighter justifying this low density as the fibres increases. However, the fibres play a second role, they create a network of pores in the matrix responsible for the increase of sample's porosity [50]. Bkarker and Heniford justify this porosity by the creation of a layer of fibres superimposed on each other and thus increasing the air layers in the material. Furthermore, the hollow structure of these fibres allows also the increase of the pore network in the matrix [51]. On the other hand, other researchers attribute this behaviour to the dry cycles apply to the composites during the curing period when the material loses water. This reduction causes a weak adhesion between the fibres and the matrix particles leaving voids at the fibre-matrix interface [45].

Apart from the percentage of fibres which is studied at 0.3% and 0.6% of the weight of the sample, two granulometries were highlighted in this work: L_{75} and L_{50}. The incorporation of equal cotton wastes in these materials with different granulometries shows that fibres have more impact on samples that have more fine particles. A deep analysis of Table 4 shows a variation of density equal to -6.67% with $L_{50}Y_8$, -7.78% with $L_{75}Y_8$ while this same variation is -3.17% with $L_{50}Y_6$ and -4.51% with $L_{75}Y_6$ when fibres content varies from 0.3 wt% to 0.6 wt%. Concerning the porosity, one can note a variation equivalent to +1.31% for $L_{50}Y_8$, +2.1% for $L_{75}Y_8$, +1.68% for $L_{50}Y_6$ and + 3.44% for $L_{75}Y_6$. Knowing that L_{75} has a more compact structure due to the size of its particles, the incorporation of fibres in its matrix will be likely to create a porous structure more easily than the one of L_{50}.

In fact, it has been shown that cellulose increases the permeability of CSH to water during a hydration process [52]. The development of this CSH phase requires a good adhesion to the fibre-matrix interface. The more the hydrated phases are formed, the more there is adsorption of cellulose and the more there is formation of a thick and highly permeable CSH [52, 53]. In a composite with more coarse particles, the degree of reactivity between the particles is lower than in a matrix with more fine particles. This is the reason why the presence of fibres has more impact (high variation of properties) in a sample of L_{75} than in the one of L_{50} on both density and porosity.

Independently of the compositions of the specimens, water absorption increases with the increasing of fibres content as it is shown in Fig. 5. It appears that $L_{75}Y_8Z_{0.3}$ has a value of water absorption of 17.62% while $L_{75}Y_8Z_{0.6}$ has 18.72%. Similar behaviour is observed for the remaining

Table 4 Density and porosity of the samples

Samples	Bulk density (kg.m^{-3})	Variation of bulk density with add of fibers content (%)	Porosity (%)	Variation of porosity with add of fibers content (%)
$L_{50}Y_8Z_{0.3}$	1.95	- 6.67	31.66	+ 1.31
$L_{50}Y_8Z_{0.6}$	1.82		32.07	
$L_{75}Y_8Z_{0.3}$	1.67	- 7.78	32.43	+ 2.1
$L_{75}Y_8Z_{0.6}$	1.54		33.12	
$L_{50}Y_6Z_{0.3}$	1.89	- 3.17	31.9	+ 1.68
$L_{50}Y_6Z_{0.6}$	1.83		32.43	
$L_{75}Y_6Z_{0.3}$	1.55	- 4.51	33.39	+ 3.44
$L_{75}Y_6Z_{0.6}$	1.48		34.58	

three specimens. It was also observed that, low water absorption corresponds to high flexural strength. These two observations lead to suggest the hypothesis that the ability of bio-composite to absorb water is linked not only to fines content and to formation of binding phases, as it is case for the ordinary laterite-cement composites [54–56] but also to the fibres content. Two reasons can explain it. On the one hand, it can be justify by the hydrophilic nature of cotton waste [57]. This property gives it an absorbent character with regard to water. On the other hand, the incorporation of fibres content gives the eco-composite a more porous nature, which allows water to penetrate the matrix when immersed in order to fill the empty spaces [24, 58].

3.2 Phases Evolution and Microstructure

3.2.1 Phases Evolution

Infrared spectra of all formulated composites (Fig. 6a, b and c) are conducted in order to investigate the chemical bonding and functional groups present within the matrix. The IR spectra of the composites without any addition of waste cotton fibres ($L_{50}Y_8Z_0$ and $L_{75}Y_8Z_0$) exhibited the bands between 3695 and 3610 cm^{-1} assigned to the OH bonds belonging to kaolinite and goethite. These OH bonds shift slightly to lower absorption bands (3682 – 3607 cm^{-1}) for the specimens $L_{50}Y_8Z_{0.3}$, $L_{50}Y_8Z_{0.6,}$ $L_{75}Y_8Z_{0.3}$ and $L_{75}Y_8Z_{0.6}$. It is observed a progressive shift of the OH bands with the addition of cement, shift enhanced with the presence of cellulose (Fig. 6). In fact, these two elements favoured the polycondensation of the aluminosilicates (CASFH and CASH) with consequent changes in the OH its chemical environment. The band situated at 1639 cm^{-1} confirmed the above-described bands. This band losses intensity with the content of cellulose (Fig. 6a and b). The fibres absorb the water due

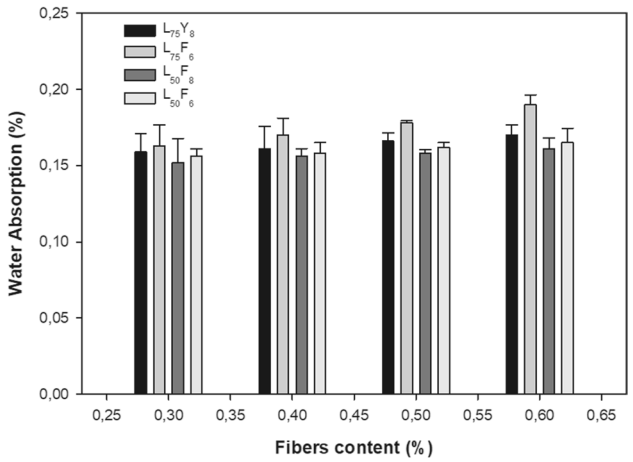

Fig. 5 Water absorption behaviour of laterite-cement composites with addition of waste cotton fibres

to their hydrophile properties resulting in the establishment of bonding with cellulosic compounds. Muthuraj et al. [58]), Seunghwan et al. [59] and Tran et al. [18] reported this similar observation.

The absorption bands between 1442 and 1436 cm^{-1}, ascribed to stretching C – O bonds, are observed with a weak intensity, indicative for the good polycondensation and chemical stability of the cementitious phases formed. The bands corresponding to the polycondensed aluminosilicates are depicted at 1031 cm^{-1} ($L_{50}Y_8Z_0$ and $L_{75}Y_8Z_0$) and at 1024 cm^{-1} ($L_{50}Y_8Z_{0.3}$, $L_{50}Y_8Z_{0.6,}$ $L7_5Y_8Z_{0.3}$ and $L7_5Y_8Z_{0.6}$). It is observed a progressive shift of the band towards low value as the consequence of the enhancement of the formation of CASFH and CASH in the presence of cellulose. Those at 995 – 400 cm^{-1} are related to the formation of CASH and suggesting the presence of fibres into the matrix does not inhibit the potential reaction that may occur. This assertion is in line with the previous research works [60, 61]. Additionally, one can say that the process used for the manufacture of samples in this works does not affect the chemical compositions of the developed eco composites as Komal et al. [62] equally affirmed.

The X-ray patterns of laterite-cement composites with 6 and 8 wt% of cement incorporating fibres at different dosages (0.3; 0.4; 0.5 and 0.6 wt%) and aged of 90 days are described in Fig. 7. These figures show the behaviour of the mineral's phases in the materials with the increase of cotton waste. The main crystalline phases identified are Gismondine (Gi) ($CaAl2Si_2O_8$-$4(H_20)$), Stratlingite (S) ($Ca_2Al_2(SiO_2)(OH)10$-$2.5H_2O$), CASFH and Hematite (He). However, Hematite is just visible on the X-ray patterns attributed to the composites without cotton waste fibre ($L_{50}Y_8Z_0$ and $L_{75}Y_8Z_0$). Hematite here appears as residual product of unreacted goethite. Its seems that the presence of cellulose improves the level of reactivity within the matrix and by the way hinder the formation hematite. The above-mentioned phases are crystalline phases that are formed in the aluminosilicates once the cement hydration reaction has taken place completely [44, 63, 64]. The improvement of the reactivity in the presence of cellulose has positive consequence on the level of crystallinity of the different binder phases developed (Fig. 7). Whether the matrix is dominated by fine particles or by coarse particles, the addition of 0.3 wt% of cotton fibres seems to make the peaks of the phases corresponding to ettringite, stratlingite and hematite disappear and to increase those relating to Gismondine and CASFH. This behaviour confirmed the catalytic role of cellulose in the cementitious reactions as some researchers found [45].

Previous works [52, 53, 65] on the behaviour of cellulose in cement matrices has shown that hydrogen bonds are likely to form with the presence of free hydroxyl groups on cellulose molecules in order to developed ordered

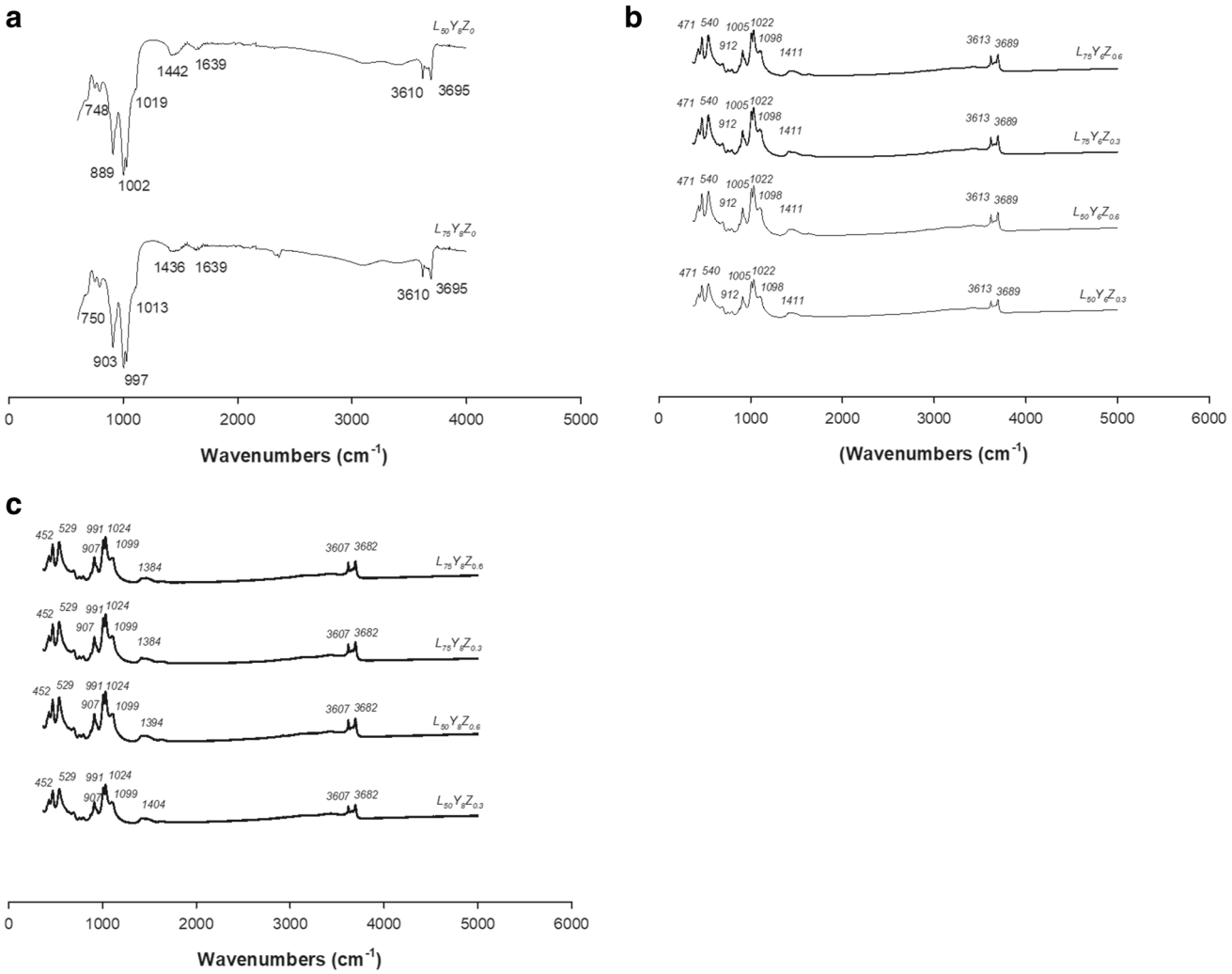

Fig. 6 FT-IR spectra of (**a**) $L_{75}Y_8Z_0$ and $L_{50}Y_8Z_0$, (**b**) different samples with 6 wt% of cement and (**c**) different samples with 8 wt% of cement content

but imperfect crystal phases. When waste cotton fibres are added from 0.3% to 0.6 wt%, one can notice a slight change in the peaks corresponding to crystalline phases in $L_{50}Y_8Z_0$ while in $L_{75}Y_8Z_0$, the crystallinity of cementitious phases become more noticeable. This may suggest that the catalytic role of cellulose is more pronounced in presence of small particles in laterite-cement composites and further justifies the variations in porosities and densities found in paragraph 2. Meriem El Boustani [65] found that the crystalline phases resulting from cellulosic reactions in cementitious matrix have a density equal to 1.59 g.cm-3^3 while those resulting only from the hydration process without the presence of cellulosic fibres are thinner and impermeable with a density of 1.55 g.cm-3^3. This further explains why the density increases with the addition of cotton fibres regardless the particle size distribution but also why a significant variation in properties of $L_{75}Y_8Z_0$ compared to $L_{50}Y_8Z_0$ is observed when the same cotton fibre content is added.

3.2.2 Microstructure

Figure 11 presents the micrographs of laterite-cement composite at low magnification when 0.3 wt% and 0.6 wt% of cotton fibre are added. It can be observed a homogenous structure in both $L_{50}Y_8Z_{0.3}$ and $L_{75}Y_8Z_{0.3}$(Fig. 8a and b) with a difference at the level of densification. $L_{75}Y_8Z_{0.3}$ seems to be denser compared to $L_{50}Y_8Z_{0.3}$ in which the cotton fibre are even well visible (Fig. 8a). This proves that fines particle size enables to embed the coarse particles and cotton fibres compared to the coarse particles that prevent the cotton fibre to be embedded.

On the Fig. 8c and d, it can be observed the detailed features of the morphology of laterite-cement composites

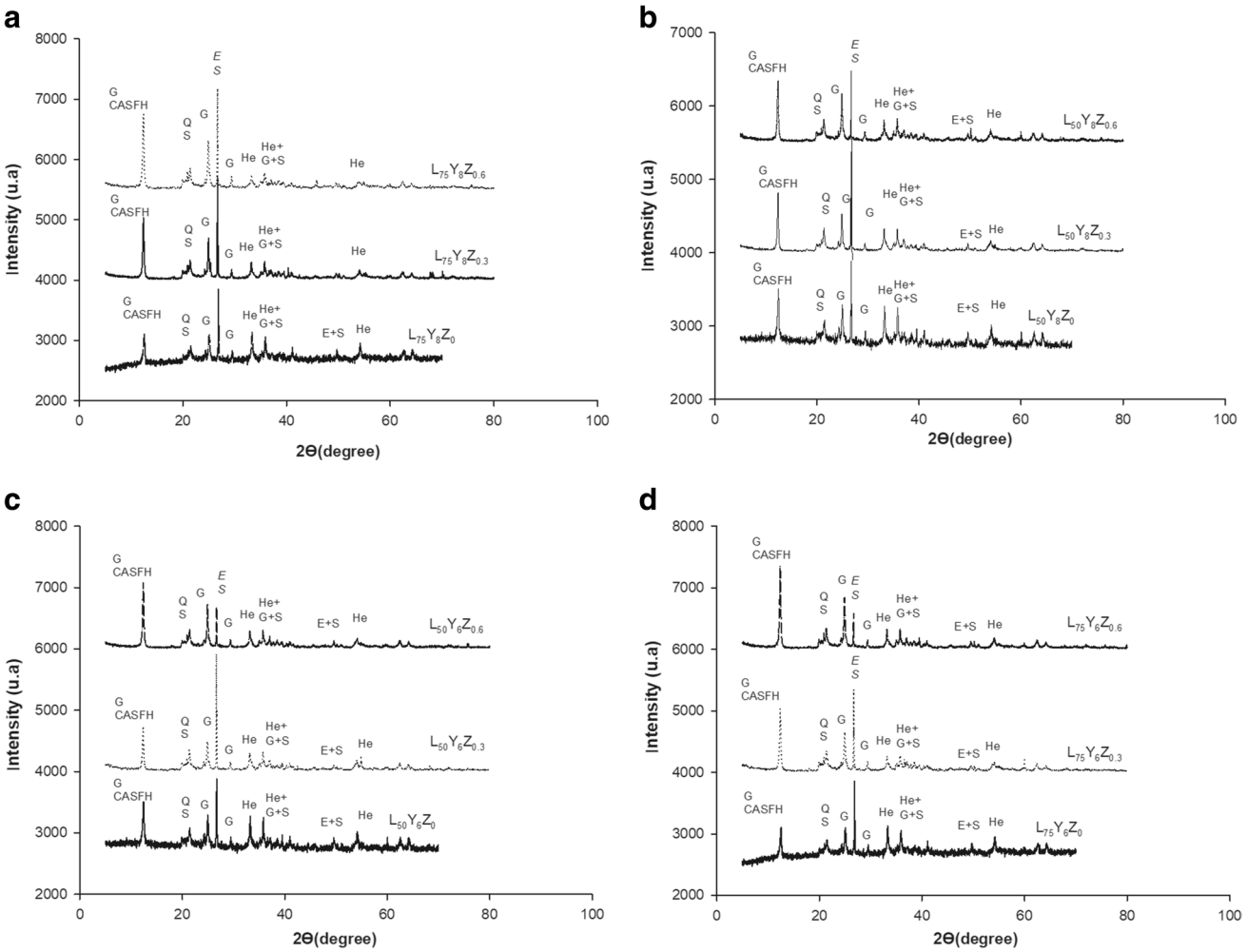

Fig. 7 FT-IR spectra at Z_0, $Z_{0.3}$ and $Z_{0.6}$ of (**a**) $L_{75}Y_8$, (**b**) $L_{75}Y_6$, (**c**) $L_{50}Y_8$, (**d**) $L_{50}Y_6$

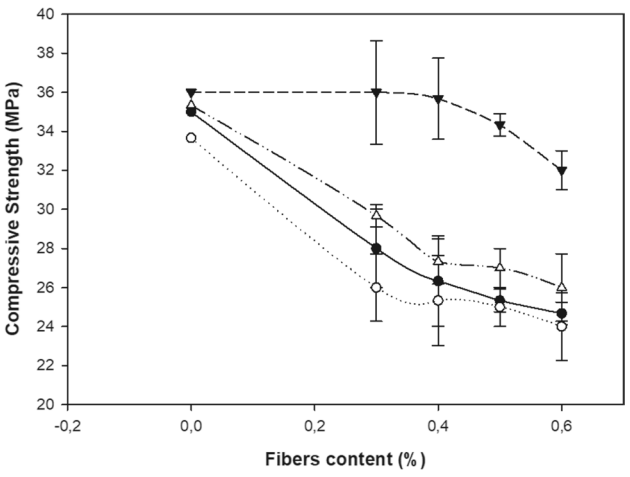

Fig. 8 ESEM Micrographs of laterite-fibres composite at low magnification of (**a**) $L_{50}Y_8Z_{0.3}$, (**b**) $L_{75}Y_8Z_{0.3}$ (**c**) $L_{50}Y_8Z_{0.6}$ and (**d**) $L_{75}Y_8Z_{0.6}$

($L_{50}Y_8Z_{0.6}$ and $L_{75}Y_8Z_{0.6}$) when the fibres within the matrix increase. According to these figures, the increase of cotton fibres modifies the microstructure of the both samples. One can observed that in Fig. 8d the pore created by the increase of fibre confirming the hypothesis that the fibre is responsible for the increase of porosity as it was demonstrated in paragraph 3.2. However, the fibre remains embebbed into the matrix compared to $L_{50}Y_8Z_{0.6}$ where one can see a series of superimposed fibres totally beside to the main matrix (Fig. 8c). This trend is in agreement with the DRX patterns where it is reported that the formation of a cementitious phases (CASFH and CASH) with the increase of fibres in $L_{75}Y_8Z_{0.6}$ is due to the good adhesion between the fibres and the matrix. In addition, this could justify the reason why the fibres have more impact in physico-mechanical properties of $L_{75}Y_8Z_0$ compared to $L_{50}Y_8Z_0$ as reported in paragraph 3.1.

However, an observation of Fig. 8c leads to confirm the fact that, between the cotton fibres and the laterite-cement composite, there is no reaction that occur. The fibre only

contributes to the increase of the reactivity of the chemical binding phases but do not take part to the reactions for the formation of these phases.

At high magnification (Fig. 9), the micrograph of specimens shows the contact between fibres and the matrix. At 0.3 wt% of fibres, one can observe in $L_{50}Y_8Z_{0.3}$ a groove leaves by the fibres which unravelled from the matrix (Fig. 9a). However, it is not the case with $L_{75}Y_8Z_{0.3}$ in which a good cohesion is still observed between the cotton fibres and the laterite-cement particles (Fig. 9b**).** At 0.6 wt% of fibres, the $L_{50}Y_8Z_{0.6}$ micrograph (Fig. 9c) shows fibres dissociated from the matrix suggesting that there is not a good adhesion between the coarse particle and fibres leading to confirm the observation made on the micrograph of Fig. 9a. The micrographs of $L_{75}Y_8Z_{0.6}$ represented on Fig. 12d shows a structure with high porosity compared to $L_{75}Y_8Z_{0.3}$ leading to confirm that more cotton fibres are added to the matrix important is the porosity. This trend is in agreement with the increase of porosity when the cotton fibres increase (Table 4).

3.3 Mechanical Properties

The variation of flexural strength is summarized in Fig. 10. The values of $L_{75}Y_8Z_0$, $L_{75}Y_6Z_0$, $L_{50}Y_8Z_0$ and $L_{50}Y_6Z_0$ (without cotton fibres) are 11,7 MPa, 9,2, MPa, 7,6 MPa and 6,4 MPa, respectively [66]. The incorporation of cellulosic fibres, within the matrix, from 0.3 wt% up to 0.6 wt%, induces a slight decrease of the flexural strength to 9,04 MPa, 8,52 MPa, 8,28 MPa and 7,88 MPa for $L_{75}Y_8Z_{0.6}$, $L_{75}Y_6Z_{0.6}$, $L_{50}Y_8Z_{0.6}$ and $L_{50}Y_6Z_{0.6,}$ respectively. The slight decrease of the flexural strength is linked to the reduction of the interparticle contacts between the cementitious materials [67]. Considering L75, the presence of cotton fibres acting as catalysator favoured the homogeneity of the microstructure. Several authors found that the presence of cellulose inhibits the formation of portlandite and delay that of CSH within a matrix [52, 68]. The absence of portlandite in the presence of cotton fibres and the enhancement of the cementitious phases would have enhanced the flexural strength of the composites. However, it should be noted that the poor density of the fibres and the intergranular porosity developed within the matrix of the composites affect the overall strength [52, 53, 68]. Similar trend is observed with the compressive strength (Fig. 14). From Fig. 11, the values of 24.67 MPa ($L_{75}Y_8Z_{0.6}$), 28 MPa ($L_{75}Y_8Z_{0.3}$), 24 MPa ($L_{75}Y_6Z_{0.6}$), 26 MPa ($L_{75}Y_6Z_{0.3}$), 32 MPa ($L_{50}Y_8Z_{0.6}$), 36 MPa ($L_{50}Y_8Z_{0.3}$), 26 MPa ($L_{50}Y_6Z_{0.6}$) and 29.67 MPa ($L_{50}Y_6Z_{0.3}$) are obtained while the values of $L_{75}Y_8Z_0$, $L_{75}Y_6Z_0$, $L_{50}Y_8Z_0$ and $L_{50}Y_6Z_0$ are respectively 37 MPa, 33.66 MPa, 38.33 MPa and 35,33 MPa [69]. The lowest compressive strength is attribute to $L_{75}Y_6Z_{0.6}$ with 24 MPa, which have the high content of fines when the highest value is attribute to $L_{50}Y_8Z_{0.3}$ with 36 MPa with a lowest fibres content. Although the fact the compressive strength is essentially linked to the particle packing, the presence of fibres in the matrix affects the interparticle contacts within the cementitious phases and by the way, decrease the compressive strength [4, 70, 71]. In fact, when coarse particles are sufficiently embedded with strong chemical bonds, as in the case of $L_{50}Y_8$, the compressive strength is enhanced.

For the laterite-cement composites with the addition of cotton fibres, the minimum flexural strength obtained is 7,88 MPa while the minimum compressive strength is

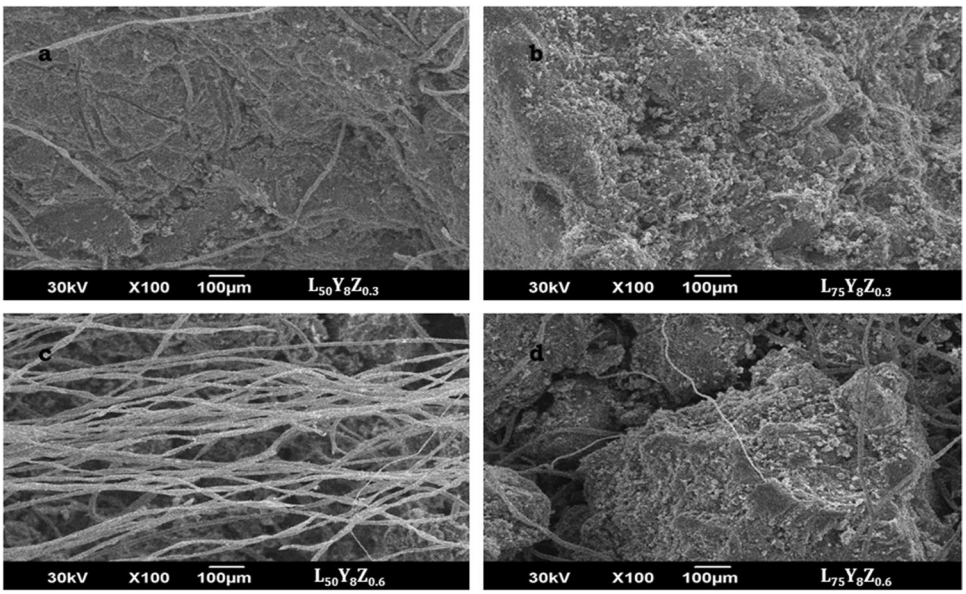

Fig. 9 ESEM Micrographs of laterite-fibres composite at high magnification of (**a**) $L_{50}Y_8Z_{0.3}$, (**b**) $L_{75}Y_8Z_{0.3}$ (**c**) $L_{50}Y_8Z_{0.6}$ and (**d**) $L_{75}Y_8Z_{0.6}$

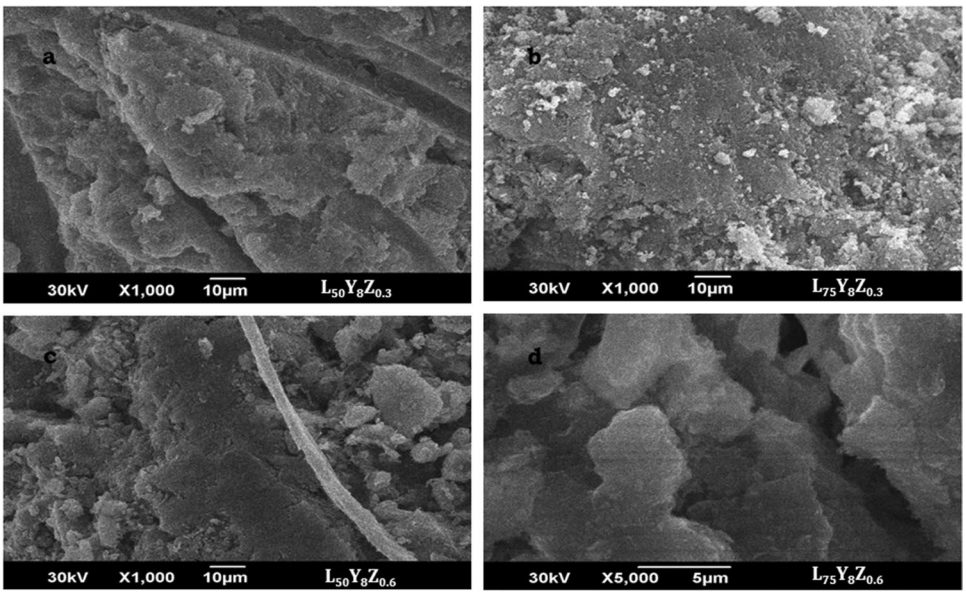

Fig. 10 Flexural strength as function of waste cotton fibres

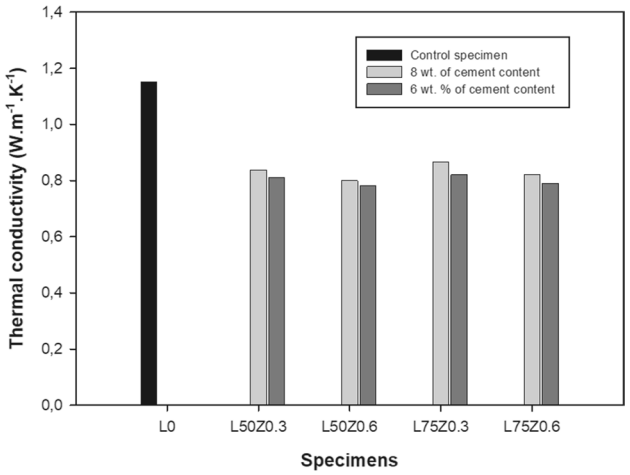

Fig. 11 Compressivestrength as function of waste cotton fibres

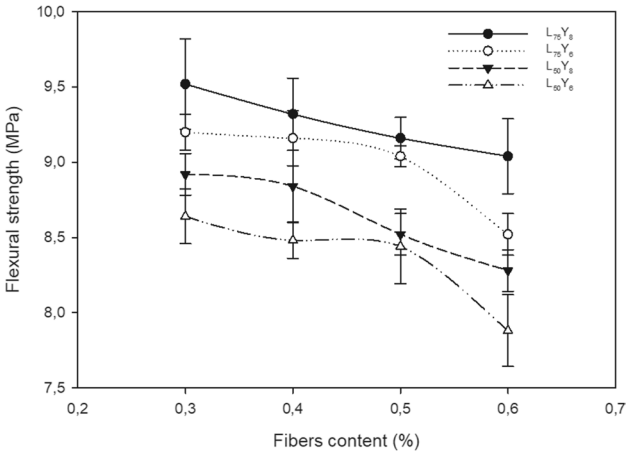

Fig. 12 Thermal conductivity of the samples as function of waste cotton fibres and cement content

24 MPa; values in accordance with the recommendations given by the international standards regarding the materials for structural applications : building systems [72].

3.4 Effect of Cotton Waste Content on Thermal Performance

Nowadays, ideal sustainable building materials should have appropriate strength for the structure, intrinsic characteristics to hinder the transfer of the thermal flux as well as noise and cold. The porous system should be efficient regarding the moisture buffering capacity (passive building system). For the laterite-cement composite under study, the mechanicals properties whatever the formulation considered are in agreement with the standard for structural applications [72].

Concerning the thermal insulation, the thermal conductivities of samples with 0.3 and 0.6 wt% of fibres content are shown in Fig. 12.

The values of thermal conductivity of $L_{50}Y_8Z_{0.3}$, $L_{50}Y_6Z_{0.3}$, $L_{75}Y_8Z_{0.3}$ and $L_{75}Y_6Z_{0.3}$ samples are respectively 0.847 $W.m^{-1}.K^{-1}$, 0.812 $W.m^{-1}.K^{-1}$, 0.866 $W.m^{-1}.K^{-1}$ and 0.82 $W.m^{-1}.K^{-1}$ while for $L_{50}Y_8Z_{0.6}$, $L_{50}Y_6Z_{0.6}$, $L_{75}Y_8Z_{0.6}$ and $L_{75}Y_6Z_{0.6}$ specimens correspond to thermal conductivity equal to 0.8 $W.m^{-1}.K^{-1}$, 0.78 $W.m^{-1}.K^{-1}$, 0.82 $W.m^{-1}.K^{-1}$ and 0.79 $W.m^{-1}.K^{-1}$. This relative low values are the results of actions of cotton fibres that reduce the thermal conductivity from about 1.1 $W.m^{-1}.K^{-1}$ [49, 73] for the standard laterite-cement composites with 0 wt% of cotton fibres to 0.78 $W.m^{-1}.K^{-1}$ for $L_{50}Y_6Z_{0.6}$. This value (0.78 $W.m^{-1}.K^{-1}$) of thermal conductivity for a building material

with a structural vocation is lower than those of conventional materials with same vocation of such as sand-cement concrete (1.5 $W.m^{-1}.K^{-1}$), steel (50 $W.m^{-1}.K^{-1}$), stone (1.8 $W.m^{-1}.K^{-1}$) [74] and remain higher than geopolymer foams [75, 76]. This behaviour could be explained by the very low thermal conductivity of waste cotton fibres ($\lambda = 0.04$ $W.m^{-1}.K^{-1}$) alone with the intra particle porosity (0.026 $W.m^{-1}.K^{-1}$) [77].

It is observed that the thermal conductivity decreases with the increase of apparent porosity linked to the increase of amount of fibres (Fig. 13) regardless of the particle size and the cement content in the matrix. The same observation was made with several various natural fibres [24, 27, 31].

However, for the same cotton waste content, the thermal conductivity of samples, which have coarser particles, is lower than those, which are dominated by fines particle [25]. From a chemical point of view, the composites with high proportion of fine particles in presence of hydrated cement likely conduct to the formation of more cementitious materials responsible for the better cohesion and compactness. Conversely, with coarse particles, having a complete reaction needs much time because of a certain distance between the surrounding of particles and its core. So, the void created between fines particles samples is necessary smaller than those of coarse particles samples. The smaller the pore size, the more difficult is for air to penetrate the matrix while the presence of air within a building material plays an important impact when insulation is concerned. Air and porosity achieve to improve insulating properties of materials due to the low thermal conductivity of air (0.026 W.m-1.K-1 at 20 °C), [77]. These results agreed with several authors who found that the higher thermal conductivity is due to the less inter porosity by the development of high compact structure [25, 31, 58].

However, the results showed that the decrease in thermal conductivity is a combination of several parameters taking into account the chemical compositions of the aggregate and fines, voids content, pore size distribution, geometry of aggregates, the type of addition and others as Mendes et al. found in their works [78]. Deep analysis of Fig. 13, leads to observe that for a total porosity of 31.66%, the conductivity is 0.83 $W.m^{-1}.K^{-1}$ in $L_{50}Y_8Z_{0.3}$ samples while in $L_{75}Y_8Z_{0.3}$, a total porosity of 32.43% induces a conductivity equal to 0.86 $W.m^{-1}.K^{-1}$. This is justified by the fact that the samples have different pore sizes due to the size distribution of the laterite aggregates in the compositions. Even if it is found by several authors that the thermal conductivity is linked to the porosity [4, 30, 79, 80], it decreases with increasing porosity (increasing fibre content) only if the materials have the same initial chemicals compositions.

Additionally, the nature of porous system can allow improving the thermal conductivity. The low values of thermal conductivity in L_{50} are the consequence of the pores connectivity more pronounced in this sample as the result of the coarse particles present that favour the interparticle porosity which are inter connected for the major part. The cumulative pores volumes of L_{75} and L_{50} are presented in Fig. 14. Gel pores (d<10nm), Capillarity pores (10<d< 100nm) and coarse pores (d>100nm) [81] can be identified. The observation of these curves shows that cumulative pores volume of L_{75} is 195.2 $mm^3.g^{-1}$ while the one of L_{50} is 123.6 $mm^3.g^{-1}$. The relatively high volume of porosity in L_{75} is link to the concentration of CSH formed in the presence of fines. Those cementitious phases are naturally porous in contrary to coarse grains of laterite that are compact and dense. Concerning the pore classes, in L_{75}, gel pores and capillary pores are present compared to L_{50} that is characterized with a higher volume of coarse pores than L_{75} (Fig. 15). The particle size distribution in L_{75} that is dominated by

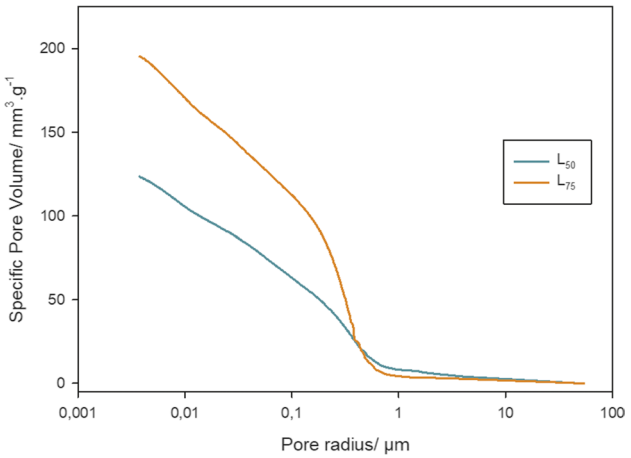

Fig. 13 Thermal conductivity of the samples as function of total porosity

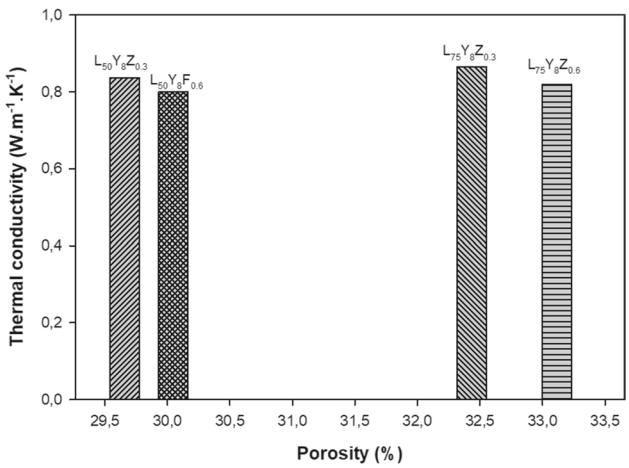

Fig. 14 Cumulative pore volume of different samples

fines leads to improve the formation of cementitious phases like CASFH and CASH. The development of these binding phases permits to achieve a good cohesion within the particles of the matrix and then, the relatively small pores.

However, in L_{50}, the quantity of coarse particles of laterite is relatively highest to prevent a good formation of cementitious phases. Therefore, there can be not enough bounder between particle and conduct to the coarse pores. The interconnectivity (responsible for good thermal conductivity) between the pores is closely linked to the coarse pores. A more a coarse pore, a better the interconnectivity. This confirm why thermal conductivity is lower in L_{50} than L_{75}.

These results of porosity and pore size distribution allow proposing L_{50} as the most promoting matrix for its moisture buffering capacity. Moisture buffering capacity is linked to the system of porosity presents in a matrix for building applications. In the laterite-cement composites, the gel pores are likely to accumulate the moisture while capillary porosity combined with coarse porosity help to regulate the desorption. Hence, in L_{50}, the balance combination of gels pores, capillary pores and coarse porosity, appear beneficial for the moisture buffering capacity as the samples present the better connectivity of pores.

4 Discussion

The quality of the building materials has an important influence on life quality, comfort and environment. Achieve sustainable construction is a great challenge in a moment where world is facing global warming potential towards climate change with the rise of temperature. In order to minimize the negative impacts of the building construction into the environment, porous laterite cement composites reinforced with cotton fibres are proposed with the intrinsic structural, technical, thermal and hygroscopic properties that respect international standards. The evaluation of the environmental impact of a construction material is generally based on the energy required for the production and its implementation. This energy includes that of the extraction of raw materials, the transportation and the process. Nowadays, the most used raw material for building construction is cement. Studies have shown that its implementation requires a large amount of energy due to the transformation of the clinker. This energy can be evaluated of about 2.38 – 5.4 MJ/kg, equivalent to about 0.8 $KgCO_2$/kg [82–84]. This is also the case for several other structural materials such as steel, traditional and advanced ceramics, whose manufacture requires a high-temperature firing process [83, 85, 86].

The environmental impact of concrete block is considerable mainly due to the manufacture of Ordinary Portland Cement (OPC), which is responsible for about 91% of its carbon emissions [87]. According to IPCC figures, the cement industry accounts for 6.97% of global CO_2 emissions. The high CO_2 emission associated with the concrete industry is partly due to the high-energy consumption of the manufacturing process, which is an energy-intensive process (T ≥1300 °C). To make 01 ton of cement, 400 kg of CO_2 is emitted into the atmosphere, which is added to the emissions associated with heating the system. In total, it is ~ 1000 kg of CO_2 that is emitted per ton of cement, thus calling for nearly 4 MJ/kg to make a sandcrete block with a thermal conductivity of 1.5 W/m.K. Hence, developing building materials that use alternative binders could produce a significant saving in cement including reduction of carbon

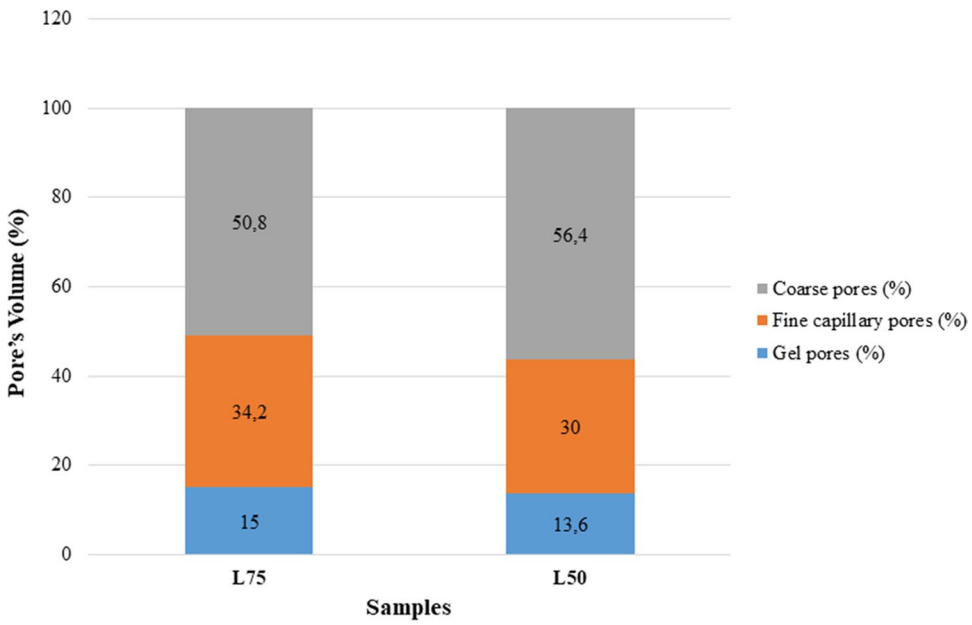

Fig. 15 Pore class distribution of samples L_{75} and L_{50}

emissions and Embodied Energy (EE) of building materials. Table 5 shows that compressed earth bricks have the lowest energy consumption, followed by cement bricks, then geopolymer and finally fired bricks. Fired brick and geopolymer are materials that do not use cement as binder. However, the processes used for their implementation remain very energy intensive. Despite the fact that Metakaolin (MK) can reduce energy consumption by half compared to cement manufacturing, the production of Sodium Silicate with its melting of sand and quartz up to 1500 °C leads to a high Carbon emissions and energy consumption of geopolymers [88, 89]. The EE of geopolymer is about 60% higher than a concrete block due to the alkali activator used to produce geopolymers (EE of NaOH = 15 MJ/kg and EE of $NaSiO_2$ = 4.6 MJ/kg) [87, 89, 90] even though its carbon emission is lower. As mentioned above, the fired bricks do not require also cement as a binder but have a very high demand of energy for their manufacture. Clay, although it is a green material, undergoes a heat treatment of up to 1200 °C for 48 h [74, 84, 91]. Thus, leading to a high EE of fired bricks compared to concrete blocks.

Although laterite is not a binder, its clay fraction (kaolinite with the structure significantly affected to being attacked/dissolved in alkaline media with consequent formation of cementitious phases as CASH and CASFH) and iron mineral content leads it to become natural concrete when adding small quantity of cement as binder [83, 92]. Thus, it does not need any pre-treatment before using and its extraction requires little or no energy. Thanks to the previous works done, the embodied energy of the laterite cement composite manufactured can estimated between 8.96 and 10.07 MJ/block with basic arithmetic rules when considering the EE of cotton fibres of about 10.5 MJ/kg [86] and EE of cement equal to 3.72 MJ/kg [83]. The data recorded in Table 5 show a decrease of at least 29% of EE with the eco composite manufactured compared to the most common used material in building. The embodied energy of this eco composite achieve to be relatively low compare to the others mentioned above as the process of its implementation doesn't requires a lot of energy. Its extraction is eco-friendly and the fact that it is generally took on the construction site permit to save the transportation energy impact. As shown in the results, aluminasilicates based cotton fibres have good hydrothermal properties compared to the others building materials thanks to its low thermal conductivity.

The conventional building materials such as cement-sand concrete, steel, stones, …does not always provide intrinsic properties (porosity, insulation, pore connectivity, hygroscopy…) necessary to ensure passive thermal comfort in buildings. Laterite cement composites have the ability to naturally regulate the air and moisture to ensure better thermal comfort in an enclosure. Moreover, with the addition of cotton fibres in the matrix, the thermal conductivity of the final composites is reduced, thus improving its thermophysical properties. With the mechanical properties largely above the standards of construction, those matrixes does not require additional porous panels and electrical equipment's (air conditioners, ventilators …) to ensure thermal comfort.

The recycling of cotton fibres waste for use in a laterite cement composite has allowed the development of a lightweight, environmentally friendly material with all the technical recommendations for use as a building material in construction.

Combining all these properties, the eco composites manufactured in this works leads to achieve good thermal comfort, small-embodied energy and low environmental impact and appears as sustainable material for building applications through a sustainable process.

Table 5 Evaluation of embodied energy of building materials

Building materials	Materials used	Process	Embodied Energy per block (MJ/block)	Embodied Carbon per block ($KgCO_2$/block)	Thermal conductivity ($W.m^{-1}.K^{-1}$)	Reference
Eco material	Laterite, cotton fibers, cement, water	drying, crushing, sieving, mixing, pressing curing	9.52	0,95 [83]	0.78	The present study
Concrete block	Cement, sand, water	drying, sieving, mixing, molding, curing	12.5	1.33 - 1.76	2.05	[88]
Fired Brick	Clay	grinding, mixing, cutting drying, firing	30 - 40	2.17 – 4.29	1.61	[87]
Alkali Activate Concrete	Metakaolin, sand, water, silicate, sodium hydroxide	drying, sieving, mixing, molding, curing	21	1,03 – 2.6	1.1	[83, 87]

5 Conclusions

The present project deals with the use of the cellulosic cotton fibres for the improvement of insulation properties of the eco-friendly structural composites: laterites cement composites based on cotton waste fibres. The influence of cellulosic fibres content, particle size of laterite and cement ratio on the thermo-mechanical, structural as well as insulating properties were investigated in details. Based on the outcomes, the following conclusions can be drawn:

- The content of cellulosic fibres namely, cotton waste fibres, greatly influences the thermal performance of the laterite-cement composites;
- The cellulosic fibres play a catalytic role for the formation of the cementitious phases including CASH and CASFH within the matrices;
- The decrease in thermal conductivity and bulk density is related to the interconnectivity between the pores, which enhance the insulating components;
- Laterite is green material having corroded kaolinite significantly affected to being attacked/dissolved in alkaline media with consequent formation of cementitious phases as CASH and CASFH;
- Optimal thermal properties of the structural composites achieved with 6 wt% cement, 0.6 wt% cotton fibres and better packing density of laterites particles (50/50) ($\lambda = 0.78$ W.m^{-1}.K^{-1}).

With regard to the minimum mechanical performance obtained in this study (7.88 MPa for flexural and 24 MPa for compressive strength respectively to $L_{50}Y_6Z_{0.6}$ and $L_{75}Y_6Z_{0.6}$), the developed eco composites are part of the range of green materials. They minimize the use of natural resources, have a low ecological impact, do not pose a risk to human health and the environment and are compatible with sustainable strategies.

Acknowledgements The authors of this article wish to acknowledge the FLAIR Fellowship African Academic of Science and the Royal Society. No. FLR/R1/201402. They also recognize the assistance of the staff of the Laboratory at the MIPROMALO for their assistance in the characterization of resulting products.

Author Contributions Van Essa L. Kamga. Samen: Conceptualization, Methodology, Investigation, Writing - original draft, Juvenal Giogetti Deutou: Validation, Writing - review & editing, Visualization, Rodrigue Cyriaque Kaze: Validation, Methodology, Writing - review & editing, Visualization, original draft. Franck Docgne Kammogne: Methodology, Writing review & editing, original draft, Pierre Meukam: review & editing, Elie Kamseu: Supervision, Methodology, Resources, C. Leonelli: Resources, Supervision.

Funding The characterization of samples was supported by Dr. Elie Kamseu, under the FLAIR fellowship of African Academic of Science and the Royal Society N° FLR/R1/201402.

Data Availability All data generated or analysed during this study are included in this article.

Code Availability Not applicable.

Declarations

This manuscript has been published elsewhere in any form or language and has not been submitted to more than one journal for simultaneous consideration.

Declaration on Conflict of Interest The authors declare that they have no conflict of interest.

Consent to Participate Note applicable.

Consent for Publication Not applicable.

Ethics Approval Not applicable.

References

1. Zhou CY, Zhong X, Liu S, Han S, Liu P (2017) Study on the relationship between thermal comfort and air-conditioning energy consumption in different cities. J Comput 28:135–143. https://doi.org/10.3966/199115592017042802010
2. Chua KJ, Chou SK, Yang WM, Yan J (2013) Achieving better energy-efficient air conditioning - A review of technologies and strategies. Appl Energy 104:87–104. https://doi.org/10.1016/j.apenergy.2012.10.037
3. Asdrubali F, Alessandro FD, Schiavoni S (2015) A review of unconventional sustainable building insulation materials. SUSMAT, 1–17. https://doi.org/10.1016/j.susmat.2015.05.002
4. Ben Mansour M, Jelidi A, Cherif AS, Ben S, Jabrallah (2016) Optimizing thermal and mechanical performance of compressed earth blocks (CEB). Constr Build Mater 104:44–51. https://doi.org/10.1016/j.conbuildmat.2015.12.024
5. Simona PL, Spiru P, Ion IV (2017) science direct increasing the energy efficiency of buildings by thermal insulation. Energy Procedia 128:393–399. https://doi.org/10.1016/j.egypro.2017.09.044
6. AIEA (2019) Rapport Annuel De L'aiea 2019. http://www.acm.gov.tn/Fr/telecharger.php?code=131
7. UNESCO, ONU-Eau (2020) Rapport mondial des Nations Unies sur la mise en valeur des ressources en eau 2020: L'eau et les changements climatiques. Paris, UNESCO: www.unwater.org/unwater-publications%2024
8. R Lydie lescarmontie, Eric Guilya, D Matthews, Sakina pen point, Bhai Rumjaun, Jenny Schlüpmann, Wilgenbus, Rapport spécial du GIEC sur le changement climatique, chapitre 8, p. 714. http://www.climatechange2013.org/images/report/WG1AR5_Chapter08_FINAL.pdf
9. WMO united in Science(2020) A multi-organization of the latest climate change information, 1–10
10. Marques DV, Barcelos RL, Silva HRT, Egert P, Parma GOC, Girotto E, Consoni D, Benavides R, Silva L, Magnago RF (2018) Recycled polyethylene terephthalate-based boards for thermal-acoustic insulation. J Clean Prod 189:251–262. https://doi.org/10.1016/j.jclepro.2018.04.069
11. Naldzhiev D, Mumovic D, Strlic M (2020) Polyurethane insulation and household products – A systematic review of their impact on indoor environmental quality. Build Environ 169:106559. https://doi.org/10.1016/j.buildenv.2019.106559

12. Khoukhi M (2018) The combined effect of heat and moisture transfer dependent thermal conductivity of polystyrene insulation material: Impact on building energy performance. Energy Build 169:228–235. https://doi.org/10.1016/j.enbuild.2018.03.055
13. Schiavoni S, D'Alessandro F, Bianchi F, Asdrubali F (2016) Insulation materials for the building sector: A review and comparative analysis. Renew Sustain Energy Rev 62:988–1011. https://doi.org/10.1016/j.rser.2016.05.045
14. Gonçalves M, Simões N, Serra C, Flores-Colen I (2020) A review of the challenges posed by the use of vacuum panels in external insulation finishing systems. Appl Energy 257:114028. https://doi.org/10.1016/j.apenergy.2019.114028
15. Mao S, Kan A, Wang N (2020) Numerical analysis and experimental investigation on thermal bridge effect of vacuum insulation panel. Appl Therm Eng 169:114980. https://doi.org/10.1016/j.applthermaleng.2020.114980
16. Jiang S, Zhang M, Jiang W, Xu Q, Yu J, Liu L, Liu L (2020) Multiscale nanocelluloses hybrid aerogels for thermal insulation: The study on mechanical and thermal properties. Carbohydr Polym 247:116701. https://doi.org/10.1016/j.carbpol.2020.116701
17. Pourghorban A, Kari BM, Solgi E (2020) Assessment of reflective insulation systems in wall application in hot-arid climates. Sustain Cities Soc 52:101734. https://doi.org/10.1016/j.scs.2019.101734
18. Tran DT, Nguyen ST, Do ND, Thai NNT, Thai QB, Huynh HKP, Nguyen VTT, Phan AN (2020) Green aerogels from rice straw for thermal, acoustic insulation and oil spill cleaning applications. Mater Chem Phys 253:123363. https://doi.org/10.1016/j.matchemphys.2020.123363
19. Wicklein B, Kocjan A, Salazar-Alvarez G, Carosio F, Camino G, Antonietti M, Bergström L (2015) Thermally insulating and fire-retardant lightweight anisotropic foams based on nanocellulose and graphene oxide. Nat Nanotechnol 10:277–283. https://doi.org/10.1038/nnano.2014.248
20. Maddalena R, Roberts JJ, Hamilton A (2018) Can Portland cement be replaced by low-carbon alternative materials? A study on the thermal properties and carbon emissions of innovative cements. J Clean Prod 186:933–942. https://doi.org/10.1016/j.jclepro.2018.02.138
21. Buratti C, Belloni E, Lascaro E, Merli F, Ricciardi P (2018) Rice husk panels for building applications: Thermal, acoustic and environmental characterization and comparison with other innovative recycled waste materials. Constr Build Mater 171:338–349. https://doi.org/10.1016/j.conbuildmat.2018.03.089
22. Mathur VK (2006) Composite materials from local resources. Constr Build Mater 20:470–477. https://doi.org/10.1016/j.conbuildmat.2005.01.031
23. Xing Q, Hao X, Lin Y, Tan H, Yang K (2019) Experimental investigation on the thermal performance of a vertical greening system with green roof in wet and cold climates during winter. Energy Build 183:105–117. https://doi.org/10.1016/j.enbuild.2018.10.038
24. Guna V, Ilangovan M, Hu C, Venkatesh K, Reddy N (2019) Valorization of sugarcane bagasse by developing completely biodegradable composites for industrial applications. Ind Crops Prod 131:25–31. https://doi.org/10.1016/j.indcrop.2019.01.011
25. Chabannes M, Bénézet JC, Clerc L, Garcia-Diaz E (2014) Use of raw rice husk as natural aggregate in a lightweight insulating concrete: An innovative application. Constr Build Mater 70:428–438. https://doi.org/10.1016/j.conbuildmat.2014.07.025
26. Wei K, Lv C, Chen M, Zhou X, Dai Z, Shen D (2015) Development and performance evaluation of a new thermal insulation material from rice straw using high frequency hot-pressing. Energy Build 87:116–122. https://doi.org/10.1016/j.enbuild.2014.11.026
27. Zou S, Li H, Wang S, Jiang R, Zou J, Zhang X, Liu L, Zhang G (2020) Experimental research on an innovative sawdust biomass-based insulation material for buildings. J Clean Prod 260:121029. https://doi.org/10.1016/j.jclepro.2020.121029
28. Shibib KS (2015) Effects of waste paper usage on thermal and mechanical properties of fired brick. Heat Mass Transf Und Stoffuebertragung. 51:685–690. https://doi.org/10.1007/s00231-014-1438-6
29. Alomayri T, Vickers L, Shaikh FUA, Low IM (2014) Mechanical properties of cotton fabric reinforced geopolymer composites at 200–1000°C. J Adv Ceram 3:184–193. https://doi.org/10.1007/s40145-014-0109-x
30. Saghrouni Z, Baillis D, Naouar N, Blal N, Jemni A (2019) Thermal properties of new insulating juncus maritimus fibrous mortar composites/experimental results and analytical laws. Appl Sci 9. https://doi.org/10.3390/app9050981
31. Belhadj B, Bederina M, Makhloufi Z, Dheilly RM, Montrelay N, Quéneudéc M (2016) Contribution to the development of a sand concrete lightened by the addition of barley straws. Constr Build Mater 113:513–522. https://doi.org/10.1016/j.conbuildmat.2016.03.067
32. Alomayri T, Shaikh FUA, Low IM (2013) Characterisation of cotton fibre-reinforced geopolymer composites. Compos Part B Eng 50:1–6. https://doi.org/10.1016/j.compositesb.2013.01.013
33. Asdrubali F, Pisello AL, D'Alessandro F, Bianchi F, Fabiani C, Cornicchia M, Rotili A (2016) Experimental and numerical characterization of innovative cardboard based panels: Thermal and acoustic performance analysis and life cycle assessment. Build Environ 95:145–159. https://doi.org/10.1016/j.buildenv.2015.09.003
34. Lacoste C, El Hage R, Bergeret A, Corn S, Lacroix P (2018) Sodium alginate adhesives as binders in wood fibers/textile waste fibers biocomposites for building insulation. Carbohydr Polym 184:1–8. https://doi.org/10.1016/j.carbpol.2017.12.019
35. Sakhare VV, Ralegaonkar RV (2017) Development and investigation of cellular light weight bio-briquette ash bricks. Clean Technol Environ Policy 19:235–242. https://doi.org/10.1007/s10098-016-1200-5
36. Mbumbia L, De Wilmars AMertens, Tirlocq J (2000) Performance characteristics of lateritic soil bricks fired at low temperatures: A case study of Cameroon. Constr Build Mater 14:121–131. https://doi.org/10.1016/S0950-0618(00)00024-6
37. Kaze CR, Venyite P, Nana A, Juvenal DN, Tchakoute HK, Rahier H, Kamseu E, Melo UC, Leonelli C (2020) Meta-halloysite to improve compactness in iron-rich laterite-based alkali activated materials. Mater Chem Phys 239:122268. https://doi.org/10.1016/j.matchemphys.2019.122268
38. Kamseu E, Kaze CR, Fekoua JNN, Melo UC, Rossignol S, Leonelli C (2020) Ferrisilicates formation during the geopolymerization of natural Fe-rich aluminosilicate precursors. Mater Chem Phys 240. https://doi.org/10.1016/j.matchemphys.2019.122062
39. Kaze CR, Djobo JNY, Nana A, Tchakoute HK, Kamseu E, Melo UC, Leonelli C, Rahier H (2018) Effect of silicate modulus on the setting, mechanical strength and microstructure of iron-rich aluminosilicate (laterite) based-geopolymer cured at room temperature. Ceram Int 44:21442–21450. https://doi.org/10.1016/j.ceramint.2018.08.205
40. Tuncer ER (1977) Engineering behaviour and classification of lateritic soils in relation to soil genesis. Int J Rock Mech Min Sci Geomech Abstr 14:40. https://doi.org/10.1016/0148-9062(77)90065-1
41. Kamtchueng BT, Onana VL, Fantong WY, Ueda A, Ntouala RF, Wongolo MH, Ndongo GB, Ze AN, Kamgang VK, Ondoa JM (2015) Geotechnical, chemical and mineralogical evaluation of lateritic soils in humid tropical area (Mfou, Central-Cameroon): Implications for road construction. Int J Geo-Eng 6:1–21. https://doi.org/10.1186/s40703-014-0001-0

42. Kaze RC, Beleuk à Moungam LM, Fonkwe Djouka ML, Nana A, Kamseu E, Chinje Melo UF, Leonelli C (2017) The corrosion of kaolinite by iron minerals and the effects on geopolymerization. Appl Clay Sci 138:48–62. https://doi.org/10.1016/j.clay.2016.12.040
43. Noël J, Djobo Y, Elimbi A, Stephan D (2020) Phase and dimensional stability of volcanic ash – based phosphate inorganic polymers at elevated temperatures. SN Appl Sci 828. https://doi.org/10.1007/s42452-020-2616-4
44. Obonyo EA, Kamseu E, Lemougna PN, Tchamba AB, Melo UC, Leonelli C (2014) A sustainable approach for the geopolymerization of natural iron-rich aluminosilicate materials. Sustainability 6:5535–5553. https://doi.org/10.3390/su6095535
45. Ardanuy M, Claramunt J, Garcıa-Hortal JA, Barra M. Fibre-matrix interactions in cement mortar composites reinforced with cellulosic fibres. Cellulose 18(2):281–289. https://doi.org/10.1007/s10570-011-9493-3
46. ASTM C373-88 (2006) Standard test method for water absorption, bulk density, apparent porosity, and apparent specific gravity of fired whiteware products
47. A. C78/C78M (2018) Standard test method for flexural strength of concrete (Using simple beam with third-point loading) 1, 1–5. https://doi.org/10.1520/C0078
48. ASTM C39/C39M - 05 (2005) Standard test method for compressive strength of cylindrical concrete specimens. ASTM Int, 1–8. https://doi.org/10.1520/C0039
49. Damfeu C (2016) Caracterisation thermophysiques des materiaux locaux d'isolation thermique de batiment et modelistion des transferts thermiques 1, These, 1–215
50. Islam S, Bhat G (2019) Environmentally-friendly thermal and acoustic insulation materials from recycled textiles. J Environ Manag 251:109536. https://doi.org/10.1016/j.jenvman.2019.109536
51. Takagi H, Kako S, Kusano K. Thermal conductivity of PLA-bamboo fibre composites. Adv Compos Mater 16(4):377–384. https://doi.org/10.1163/156855107782325186
52. Pourchez J, Grosseau P, Ruot B (2010) Cement and concrete research changes in C 3 S hydration in the presence of cellulose ethers. Cem Concr Res 40:179–188. https://doi.org/10.1016/j.cemconres.2009.10.008
53. Müller VI (2006) Influence of cellulose ethers of the kintecics or early portland cement hydration. Thesis dissertation, Universitätsverlag Karlsruhe, pp 1–124
54. Kasthurba AK, Reddy KR, Venkat Reddy D (2014) Use of Laterite as a sustainable building material in developing countries. Int J Earth Sci Eng 7:1251–1258
55. Kasthurba AK, Santhanam M, Achyuthan H (2008) Investigation of laterite stones for building purpose from Malabar region, Kerala, SW India - Chemical analysis and microstructure studies. Constr Build Mater 22:2400–2408. https://doi.org/10.1016/j.conbuildmat.2006.12.003
56. Kasthurba AK, Santhanam M, Mathews MS (2007) Investigation of laterite stones for building purpose from Malabar region, Kerala state, SW India - Part 1: Field studies and profile characterisation. Constr Build Mater 21:73–82. https://doi.org/10.1016/j.conbuildmat.2005.07.006
57. Alomayri T, Assaedi H, Shaikh FUA, Low IM (2014) Effect of water absorption on the mechanical properties of cotton fabric-reinforced geopolymer composites. J Asian Ceram Soc 2:223–230. https://doi.org/10.1016/j.jascer.2014.05.005
58. Muthuraj R, Lacoste C, Lacroix P, Bergeret A (2019) Industrial crops & products sustainable thermal insulation biocomposites from rice husk, wheat husk, wood fibers and textile waste fibers: Elaboration and performances evaluation. Ind Crop Prod 135:238–245. https://doi.org/10.1016/j.indcrop.2019.04.053
59. Wi S, Park JH, Kim YU, Yang S, Kim S (2020) Thermal, hygric, and environmental performance evaluation of thermal insulation materials for their sustainable utilization in buildings. Environ Pollut 116033. https://doi.org/10.1016/j.envpol.2020.116033
60. Kapeluszna E, Kotwica Ł, Różycka A, Gołek Ł (2017) Incorporation of Al in C-A-S-H gels with various Ca/Si and Al/Si ratio: Microstructural and structural characteristics with DTA/TG, XRD, FTIR and TEM analysis. Constr Build Mater 155:643–653. https://doi.org/10.1016/j.conbuildmat.2017.08.091
61. Latifi N, Eisazadeh A, Marto A (2014) Strength behavior and microstructural characteristics of tropical laterite soil treated with sodium silicate-based liquid stabilizer. Environ Earth Sci 72:91–98. https://doi.org/10.1007/s12665-013-2939-1
62. Komal UK, Lila MK, Singh I. PLA/banana fiber based sustainable biocomposites: A manufacturing perspective, Elsevier Ltd. Compos Part B: Eng 180:107535. https://doi.org/10.1016/j.compositesb.2019.107535
63. Bouras BF, Tapsoba N, Martin M, Sabio S, Jacquet A, Beck K, Belayachi N, Bouasker M, Al-mukhtar M (2020) Effect of hydrated lime and cement on the engineering behavior of highly expansive clay 7, 1–14
64. Jaritngam S, Somchainuek O, Taneerananon P (2014) Feasibility of laterite-cement mixture as pavement base course aggregate. Iran J Sci Technol - Trans Civ Eng 38:275–284
65. El Boustani M (2016) Modification des fibres végétales par un procédé Écologique: effets sur la microstructure et la compatibilité avec les matrices polymériques. Thèse PhD, cotutelle de l'Université Cadi Ayyad et de l'Université du Québec à Trois-Rivières (2016), pp 1–229. https://depot-e.uqtr.ca/id/eprint/7970
66. Samen VELK, Kaze RC, Deutou Nemaleu JG, Tchakoute HK, Meukam P, Kamseu E, Leonelli C (2021) Engineering properties, phase evolution and microstructure of the iron-rich aluminosilicates-cement based composites: Cleaner production of energy efficient and sustainable materials. Clean Mater 1:100017. https://doi.org/10.1016/j.clema.2021.100017
67. Araya-letelier G, Concha-riedel J, Antico FC, Valdés C, Cáceres G (2018) Influence of natural fiber dosage and length on adobe mixes damage-mechanical behavior. Constr Build Mater 174:645–655. https://doi.org/10.1016/j.conbuildmat.2018.04.151
68. Pourchez J, Govin A, Grosseau P, Guyonnet R, Guilhot B, Ruot B (2006) Alkaline stability of cellulose ethers and impact of their degradation products on cement hydration. Cem Concr Res 36:1252–1256. https://doi.org/10.1016/j.cemconres.2006.03.028
69. Chen G, Lee H, Lun K, Lock P, Wong A, Tao T, Keung K (2002) Glass recycling in cement production — an innovative approach. Waste Management 22(7):747–753. https://doi.org/10.1016/S0956-053X(02)00047-8
70. Sadrolodabaee P, Claramunt J, Ardanuy M, De A (2021) Case studies in construction materials mechanical and durability characterization of a new textile waste micro- fi ber reinforced cement composite for building applications. Case Stud Constr Mater 14:e00492. https://doi.org/10.1016/j.cscm.2021.e00492
71. Zak P, Ashour T, Korjenic A, Korjenic S, Wu W (2016) The influence of natural reinforcement fibers, gypsum and cement on compressive strength of earth bricks materials. Constr Build Mater 106:179–188. https://doi.org/10.1016/j.conbuildmat.2015.12.031
72. Mulyadi A (2017) Effect of water curing duration on strength behaviour of portland composite cement (PCC) mortar Effect of water curing duration on strength behaviour of portland composite cement (PCC) mortar. https://doi.org/10.1088/1757-899X/271/1/012018
73. Meukam P (2004) Valorisation des briques de terre stabilisées en vue de l'isolation thermique de bâtiments
74. Hammond G, Jones C, Lowrie EF, Tse P (2011) The inventory of carbon and energy

75. Shi J, Liu B, Liu Y, Wang E, He Z, Xu H, Ren X (2020) Preparation and characterization of lightweight aggregate foamed geopolymer concretes aerated using hydrogen peroxide. Constr Build Mater 256:119442. https://doi.org/10.1016/j.conbuildmat.2020.119442
76. Shi J, Liu B, He Z, Liu Y, Jiang J, Xiong T, Shi J (2021) A green ultra-lightweight chemically foamed concrete for building exterior: A feasibility study. J Clean Prod 288:125085. https://doi.org/10.1016/j.jclepro.2020.125085
77. Smith DS (2013) Thermal conductivity of porous materials. https://doi.org/10.1557/jmr.2013.179
78. Mendes JC, Barreto RR, Carolina A, De Paula B, Pereira F, Brigolini GJ, André R, Peixoto F (2019) On the relationship between morphology and thermal conductivity of cement-based composites. Cem Concr Compos 104:103365. https://doi.org/10.1016/j.cemconcomp.2019.103365
79. Binici H, Eken M, Dolaz M, Aksogan O, Kara M (2014) An environmentally friendly thermal insulation material from sunflower stalk, textile waste and stubble fibres. Constr Build Mater 51:24–33. https://doi.org/10.1016/j.conbuildmat.2013.10.038
80. Burger N, Laachachi A, Ferriol M, Lutz M, Toniazzo V, Ruch D (2016) Progress in polymer science review of thermal conductivity in composites: Mechanisms, parameters and theory. Prog Polym Sci 61:1–28. https://doi.org/10.1016/j.progpolymsci.2016.05.001
81. Coppola B, Tardivat C, Richaud S, Tulliani JM, Montanaro L, Palmero P (2020) Alkali-activated refractory wastes exposed to high temperatures: development and characterization. J Eur Ceram Soc 40:3314–3326. https://doi.org/10.1016/j.jeurceramsoc.2020.02.052
82. Feiz R, Ammenberg J, Baas L, Eklund M, Helgstrand A, Marshall R (2014) Improving the CO 2 performance of cement, part I: utilizing life-cycle assessment and key performance indicators to assess development within the cement industry. J Clean Prod. https://doi.org/10.1016/j.jclepro.2014.01.083
83. Praseeda KI, Reddy BVV, Mani M (2015) Embodied energy assessment of building materials in India using process and input – output analysis. Energy Build 86:677–686. https://doi.org/10.1016/j.enbuild.2014.10.042
84. Pavia S (2020) Properties of unfired, illitic-clay bricks for sustainable construction. Constr Build Mater 121118. https://doi.org/10.1016/j.conbuildmat.2020.121118
85. Hammond GP, Jones CI (2008) Embodied energy and carbon in construction materials: 87–98. https://doi.org/10.1680/ener.2008.161.2.87
86. Bribián IZ, Capilla AV, Usón AA (2011) Life cycle assessment of building materials: Comparative analysis of energy and environmental impacts and evaluation of the eco-efficiency improvement potential. Build Environ 46:1133–1140. https://doi.org/10.1016/j.buildenv.2010.12.002
87. Dahmen J, Kim J, Ouellet-Plamondon CM (2018) Life cycle assessment of emergent masonry blocks. J Clean Prod 171:1622–1637. https://doi.org/10.1016/j.jclepro.2017.10.044
88. Habert G, Billard C, Rossi P, Chen C, Roussel N (2010) Cement and concrete research cement production technology improvement compared to factor 4 objectives. Cem Concr Res 40:820–826. https://doi.org/10.1016/j.cemconres.2009.09.031
89. Abbas R, Aly M, Hanaa K, Elkhoshkhany YGN (2020) Preparation of geopolymer concrete using Egyptian kaolin clay and the study of its environmental effects and economic cost. Clean Technol Environ Policy 22:669–687. https://doi.org/10.1007/s10098-020-01811-4
90. Adesina A (2021) Resources, environment and sustainability performance and sustainability overview of sodium carbonate activated slag materials cured at ambient temperature. Resour Environ Sustain 3:100016. https://doi.org/10.1016/j.resenv.2021.100016
91. Maskell D, Heath A, Walker P (2014) Comparing the environmental impact of stabilisers for unfired earth construction, 600:132–143. https://doi.org/10.4028/www.scientific.net/KEM.600.132
92. Van Damme H, Houben H (2018) Cement and concrete research earth concrete. Stabilization revisited. Cem Concr Res 114:90–102. https://doi.org/10.1016/j.cemconres.2017.02.035